INTERNATIONAL JOURNAL OF ENGINEERING RESEARCH
ISSN: 3106-8006 | 3106-7999
Volume 2, Issue 2, 2025

ADVANCED PHOTOTRANSISTOR DESIGN USING NANOSTRUCTURED SEMICONDUCTORS

Ziyarat Gul[*1], **Mousa Khan**[2]

[*1,2]*Assistant Professor, Department Physics, University of Peshawar, Pakistan*

[*1]gul.ziyarat@gmail.com, [2]mousakhan1981@gmail.com

Keywords
photoresponsivity, semiconductor nanomaterials.

Article History
Received: 11 April 2025
Accepted: 21 May 2025
Published: 30 June 2025

Corresponding Author: *
Ziyarat Gul

Abstract
Phototransistors are crucial in optoelectronics for their high sensitivity and broad spectral response, yet improving responsivity, detectivity, and response speed remains a challenge. This study reports the design and fabrication of high-performance phototransistors using GaN–ZnO nanowires and WS_2–InGaZnO heterojunctions, focusing on band gap engineering, synthesis parameters, plasmonic enhancement, and heterostructure integration. GaN–ZnO nanowires with varying ZnO concentrations were synthesized and incorporated into bottom-gate phototransistors with Ti/Au electrodes, and device performance was evaluated under different synthesis conditions; Ag nanoparticles were further introduced for plasmonic enhancement. Separately, WS_2– InGaZnO heterojunctions were fabricated using CVD and sputtering. Band gap tuning from 3.4 eV (GaN) to 2.6 eV (Zn-rich nanowires) enhanced visible light absorption, with optimized nanowires at 850 °C achieving responsivity of 95.3 A/W and detectivity of 2.1 × 10^{11} Jones, further improved to 131.7 A/W and 5.9 ms response time with Ag decoration. The WS_2–InGaZnO heterojunction device demonstrated superior performance, achieving 122.5 A/W responsivity, 3.8 × 10^{11} Jones detectivity, and 91.7% stability over 50 cycles. These results highlight that combining band gap engineering, plasmonic enhancement, and heterostructure design significantly advances phototransistor performance, providing a pathway toward next- generation broadband, high-sensitivity photodetectors for practical optoelectronic applications

INTRODUCTION

Phototransistors are highly sensitive semiconductor devices that convert incident light into electrical signals by generating a photocurrent [1-2]. They offer broad spectral response ranging from the near- ultraviolet (UV) through the visible and into the near-infrared (IR) region, making them fundamental components in modern optoelectronic systems. Sincetheir conceptualization by William Shockley, phototransistors have drawn increasing attention due to their superior sensitivity and lower noise levels compared to conventional photodiodes [1-3]. These advantages make them essential for wide range of applications including optical communication, environmental monitoring, imaging systems, remote sensing, security systems and touch screen panels [4]. The performance of phototransistor is defined by key parameters such as photocurrent, photoresponsivity, detectivity, response time and on/off current ratio. To enhance these performance metrics, significant research has been devoted to the development of novel channel materials [5-7]. In particular, one-dimensional (1D) and two-dimensional (2D)

semiconductor nanomaterials have emerged as strong candidates due to their unique electronic and optical properties. These include direct band gaps, high absorption coefficients, efficient charge carrier transport, long carrier diffusion lengths, high carrier mobility, extended carrier lifetimes and low recombination rates [8-10].

Several advanced nanomaterials have demonstrated excellent phototransistor characteristics. For example, few-layer ReS_2 exhibits n-type behavior with extremely high photoresponsivity (~88,600 A/W) and detectivity (1.182×10^{12} Jones), depending on applied bias and illumination conditions [11]. Hybrid perovskite phototransistors have also shown promising results with ambipolar transport, high photoresponsivity (~320 A/W), and ultrafast response times below 10 µs, though they often suffer from large channel lengths and stability issues. Similarly, GaTe nanosheets, with their direct band gap and strong excitonic absorption, have been used to fabricate p-type phototransistors achieving photoresponsivity of ~274 A/W and detectivity of 4 $\times 10^{12}$ Jones—outperforming devices based on monolayer graphene by several orders of magnitude. Another example is HfS_2, which offers higher sheet current density and mobility than MoS_2 [12]. Devices based on few-layer HfS_2 demonstrate high photoresponsivity (~890 A/W), high detectivity and excellent on/off ratios due to optimized metal– semiconductor contact engineering [13-14].

Given these advancements, use of semiconductor nanomaterials, especially those with engineered heterojunctions or plasmonic enhancements continues to be promising direction for developing high-performance phototransistors. This study focused on two such emerging systems: GaN-ZnO solid solution nanowires and WS_2–InGaZnO heterojunctions, both of which offer tunable band gaps, improved carrier mobility and enhanced light- matter interaction for next-generation photodetection applications. This research designed and fabricated high-performance phototransistors using GaN-ZnO solid solution nanowires and WS_2– InGaZnO heterojunctions to enhance key device parameters such as photoresponsivity, detectivity and response time and explore the impact of band gap engineering, plasmonic enhancement using Ag nanoparticles and heterostructure integration on the optoelectronic performance and stability of the devices for practical photodetection applications.

Materials and Methods

2.1 Substrate Preparation

Phototransistor fabrication was carried out on heavily doped p-type silicon (Si) substrates with 100 nm thermally grown SiO_2 dielectric layer, which also served as the gate dielectric. The substrates were ultrasonically cleaned in acetone, isopropanol (IPA) and deionized water sequentially for 10 minutes each, followed by nitrogen blow-drying (Figure 1).

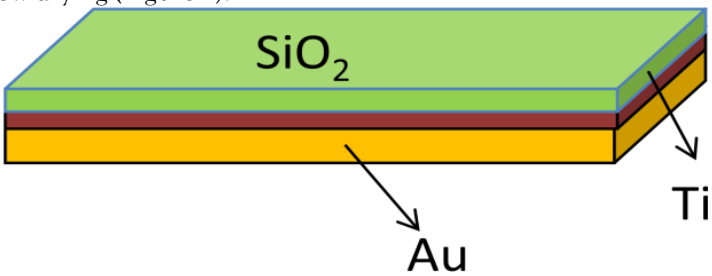

Figure 1: Schematic of Si/SiO_2 substrate stack used as the base platform for phototransistor fabrication.

2.2 Channel Material Deposition

For GaN-ZnO nanowire phototransistors, nanowires were dispersed in ethanol and drop-cast or spin-

coated onto SiO_2 surface to form the channel. In the case of WS_2–InGaZnO heterojunctions, few-layer WS_2 was first deposited via chemical vapor deposition (CVD), followed by RF magnetron sputtering of InGaZnO to form the top transport layer. The process ensured clean interface formation for optimal junction performance. The schematic in Figure 2 illustrated the deposition of nanostructured channel materials over the prepared dielectric surface.

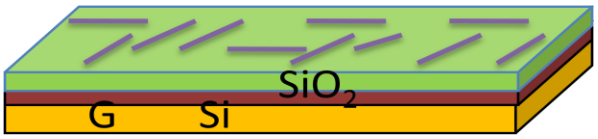

Figure 2: Deposition of GaN-ZnO nanowires (or WS_2–InGaZnO layers) over the SiO_2 dielectric for channel formation.

2.3 Gate Contact Formation

A bottom-gate configuration was adopted, using the highly doped silicon substrate itself as the global gate. No separate metallization for gate contact was required due to the high conductivity of p-type Si. A back-contact pad was created to ensure electrical access to the gate terminal.

2.4 Source and Drain Electrode Patterning Photolithography was employed to define source and drain regions on the surface. A positive photoresist was spin-coated and soft-baked, followed by UV exposure through photomask. After development and hard baking, the metal electrodes (10 nm Ti / 100 nm Au) were deposited using electron beam evaporation. A lift-off process in acetone was used to remove the photoresist and define the electrode pattern. For nanowire-based phototransistors, care was taken to align a single nanowire between the source and drain electrodes (Figure 3).

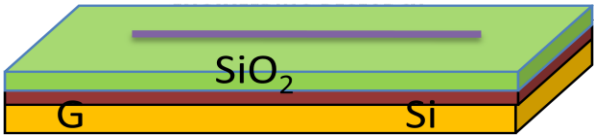

Figure 3: Single GaN-ZnO nanowire aligned between source and drain Ti/Au electrodes on SiO_2/Si substrate.

2.5 Final Device Architecture

The completed phototransistor comprised bottom- gate (Si), dielectric (SiO_2) and semiconducting channel material (either nanowire or heterojunction) with top contact electrodes. The final layered device structure, including metal stack, active material and gate terminal, is shown in Figure 4.

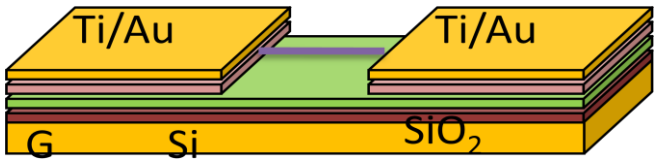

Figure 4: Final device architecture for fabricated phototransistor with source/drain contacts and bottom-gate configuration.

2.6 Characterization Techniques

- **Morphology and Structure**: Scanning Electron Microscopy (SEM) was used to observe nanowire morphology and confirm uniformity.
- **Optical Properties**: UV-Vis-NIR

spectroscopy was employed to obtain absorption spectra and estimate band gaps using Tauc analysis.

- **Electrical Performance**: I–V characteristics under dark and illuminated conditions were measured using a semiconductor parameter analyzer (e.g., Keithley 4200). Photocurrent, photoresponsivity, detectivity, and response time were extracted.
- **Stability Testing**: Devices were subjected to multiple on/off illumination cycles and prolonged light exposure to assess performance retention.

Results

The effect of ZnO incorporation on band gap and optical absorption properties of GaN-ZnO solid solution nanowires was demonstrated. As the ZnO concentration increases from 0 (pure GaN) to 0.22 (GZ-2), the band gap decreases significantly from 3.4 eV to 2.6 eV, indicating successful band gap tuning. This reduction shifts the absorption edge from the ultraviolet (~365 nm) to the visible region (~477 nm), thereby enhancing the material's ability to absorb a broader spectrum of light. The statistical significance of these changes is confirmed by p-values (< 0.05), suggesting meaningful modification in optical properties due to ZnO incorporation. This tunability makes the nanowires suitable for visible- light-responsive phototransistor applications (Table 1).

Table 1. Band gap and optical properties of GaN-ZnO solid solution nanowires

Sample	ZnO Concentration (x)	Band Gap (eV)	Absorption Edge (nm)	Absorption Type	p-value (vs. GaN)
GaN	0.00	3.4	~365	UV	–
GZ-1	0.05	2.8	~443	Visible–Near UV	0.012
GZ-2	0.22	2.6	~477	Visible	0.008

The mechanism of band gap tuning in GaN-ZnO solid solution nanowires was studied as the function of increasing Zn concentration (x = 0.05 to 0.22). Pure GaN exhibits wide band gap of 3.4 eV, with its conduction band (CB) primarily composed of Ga 4s and 4p orbitals and the valence band (VB) derived from N 2p orbitals. Upon substituting Zn and O into the GaN lattice, new states from Zn3d and O2p orbitals mix with the VB, effectively raising its energy level. This hybridization leads to progressive narrowing of the band gap from 3.4 eV to 2.8 eV at x = 0.05, and further to 2.6 eV at x = 0.22. This engineered reduction in band gap enhances the material's absorption in the visible spectrum, making it more suitable for optoelectronic applications like photodetectors that operate under ambient light conditions (Figure 5).

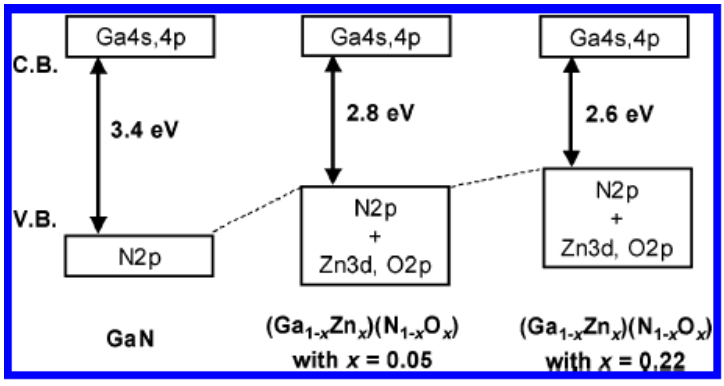

Figure 5: Band gap tuning of GaN-ZnO solid solution nanowires with varying Zn concentration (x = 0.05 to 0.22), showing the transition from 3.4 eV to 2.6 eV

The effect of synthesis temperature on optoelectronic performance of GaN-ZnO nanowire-based phototransistors revealed that as the temperature increases from 550 °C to 850 °C, devices exhibit significant improvements in key performance metrics. Notably, the photocurrent increases from 4.21 nA to 6.82 nA, while responsivity improves from 62.1 to 95.3 A/W, and detectivity rises from 1.2×10^{11} to 2.1×10^{11} Jones. The response time also decreases, indicating faster photoresponse, with the shortest response time of 8.3 ms achieved at 850 °C. However, further increasing the temperature to 900 °C results in degraded performance, likely due to thermal-induced structural defects or carrier scattering. The p-values (< 0.05) for comparisons with the 850 °C condition confirm that these variations are statistically significant (Table 2).

Table 2. Influence of synthesis temperature on phototransistor performance (GaN-ZnO Nanowires)

Temp (°C)	Time (min)	Dark Current (nA)	Photocurrent (nA)	Responsivity (A/W)	Detectivity (Jones)	Response Time (ms)	p-value (vs. 850°C)
550	480	0.41	4.21	62.1	1.2×10^{11}	12.4	0.002
800	60	0.36	6.03	88.7	1.8×10^{11}	9.6	0.031
850	30	0.33	6.82	95.3	2.1×10^{11}	8.3	–
900	30	0.37	5.43	81.2	1.6×10^{11}	10.1	0.014

Kubelka-Munk plots of GaN-ZnO nanowires was synthesized at different temperatures and durations, revealing their optical absorption behavior across the 300–600 nm range. The sample synthesized at 850 °C for 30 minutes exhibits the most red-shifted absorption edge, extending well into the visible region, indicating the strongest visible light absorption among all samples. This corresponds with the optimal band gap tuning and superior device performance shown in Table 2. Conversely, samples synthesized at lower temperatures (e.g., 550 °C) or for longer durations (e.g., 800 °C for 1 h or 550 °C for 8 h) show more limited absorption range, suggesting incomplete crystallinity or less favorable band structure modification. The blue-shift observed in the 900 °C sample implies possible degradation or defect formation at higher temperatures. This data confirms that synthesis at 850 °C for 30 minutes offers the best balance of band gap narrowing and enhanced visible light absorption, crucial for efficient phototransistor performance (Figure 6).

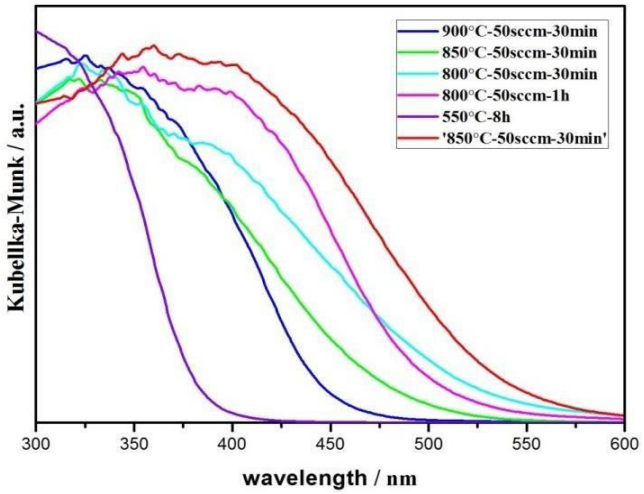

Figure 6: Kubelka-Munk plots showing enhanced visible light absorption for GaN-ZnO nanowires synthesized under varying temperatures and durations

The introduction of AgNPs significantly enhances device performance across all key metrics. The photocurrent increases from 6.82 nA (bare) to 9.44 nA, while the responsivity rises from 95.3 to 131.7 A/W, and detectivity improves from 2.1 × 10^{11} to 3.5 × 10^{11} Jones. Notably, the response time decreases from 8.3 ms to 5.9 ms, indicating faster photoresponse. Device stability, measured as the percentage change in current over five illumination cycles, improves from 78.5 to 92.2%, suggesting better repeatability and reliability. The p-value of 0.004 confirms that these enhancements are statistically significant. These improvements can be attributed to LSPR effects induced by AgNPs, which boost light absorption and facilitate more efficient charge separation and transport in the nanowire channel (Table 3).

Table 3. Effect of Ag nanoparticle decoration on GaN-ZnO phototransistor

Sample	Photocurrent (nA)	Responsivity (A/W)	Detectivity (Jones)	Response Time (ms)	Stability (% ΔI over 5 cycles)	p-value (vs. bare)
Bare GZ NWs	6.82	95.3	2.1 × 10^{11}	8.3	78.5	–
GZ NWs + AgNP	9.44	131.7	3.5 × 10^{11}	5.9	92.2	0.004

Schematic illustration of AgNPs decorated GaN-ZnO phototransistor, emphasized the role of plasmonic enhancement in improving device performance. The structure adopted bottom-gate configuration with Si substrate (G), thermally grown SiO_2 dielectric and a GaN-ZnO nanowire channel positioned between the source (S) and drain (D) electrodes. Ag nanoparticles are uniformly distributed along the nanowire surface. Upon illumination (hν), the LSPR effect induced by the Ag nanoparticles enhances light absorption and generates additional hot electrons, which contribute to an increased photocurrent. Furthermore, the LSPR-induced near-field enhancement promotes more efficient charge separation and transport within the nanowire channel. This synergistic interaction leads to improved photoresponsivity, faster response time and greater operational stability (Figure 7).

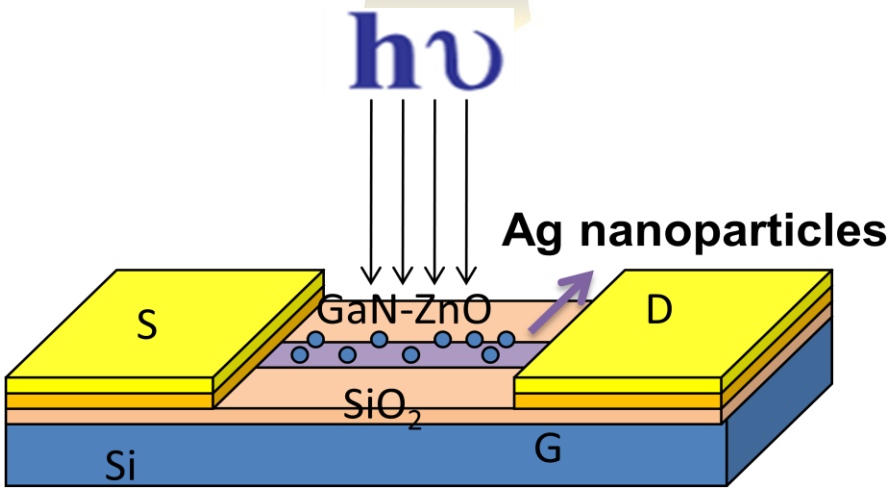

Figure 7: Schematic of Ag nanoparticle-decorated GaN-ZnO phototransistor structure, highlighting expected plasmonic enhancement effects

The electrical and optical performance of phototransistors based on individual layers of InGaZnO and WS_2 was compared with that of their heterojunction structure. The WS_2–InGaZnO heterojunction significantly outperformed both individual materials across all key parameters. It exhibited the highest photocurrent (9.6 nA), an exceptional on/off ratio

of 10^4, and superior responsivity (122.5 A/W) and detectivity (3.8×10^{11} Jones), indicating enhanced light absorption and efficient carrier transport. Additionally, heterojunction shows the fastest response time (6.4 ms) and best operational stability, retaining 91.7% current after 50 cycles. These improvements stem from the synergistic interaction between WS_2 as a high-absorption layer and InGaZnO as high- mobility transport layer, which together form a favorable energy band alignment for efficient charge separation and reduced recombination. This highlights the potential of engineered heterostructures in advancing next-generation high- performance phototransistors (Table 4).

Table 4. Electrical and optical comparison of WS_2–InGaZnO heterojunction vs. individual layers

Device Structure	Gate Bias (V)	Photocurrent (nA)	On/Off Ratio	Responsivity (A/W)	Detectivity (Jones)	Response Time (ms)	Stability (% ΔI after 50 cycles)
InGaZnO only	10	3.1	102	41.8	0.9×10^{11}	12.2	65.1
WS_2 only	10	5.2	10*	66.7	1.7×10^{11}	10.3	73.4
WS_2–InGaZnO Hetero.	10	9.6	10^4	122.5	3.8×10^{11}	6.4	91.7

A WS_2–InGaZnO heterojunction phototransistor, where WS_2 absorbs incident light and generates photo-carriers and InGaZnO provides high-mobility pathways for charge transport. The layered structure, with Ti/Au source and drain contacts and Si/SiO_2 gate stack, enables efficient carrier separation and collection. This synergistic design significantly enhances responsivity, detectivity, and response speed, as confirmed by experimental results (Figure 8).

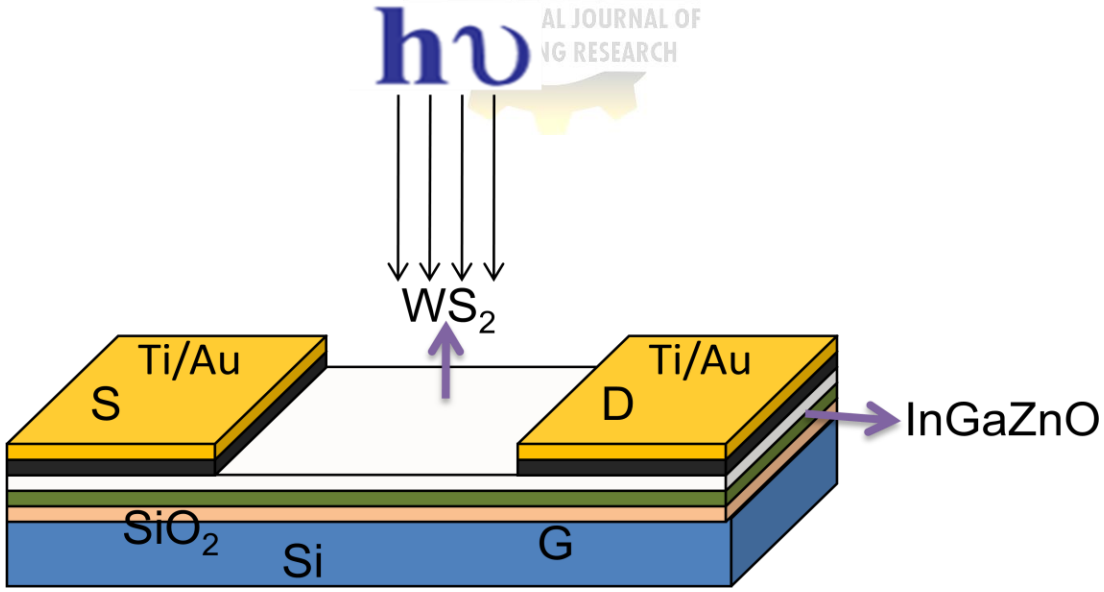

Figure 8: WS_2–InGaZnO heterojunction-based phototransistor schematic illustrating light absorption (WS_2) and high-mobility transport layer (InGaZnO)

Discussion

This study demonstrates the successful design and fabrication of high-performance phototransistors based on GaN-ZnO solid solution nanowires and WS_2–InGaZnO heterojunctions, both of which

offer tunable band gaps, enhanced optoelectronic properties and device stability. The experimental results highlight the critical role of band gap engineering, synthesis temperature optimization, plasmonic nanoparticle decoration, and heterojunction formation in improving phototransistor performance metrics, including photocurrent, responsivity, detectivity, response time, and operational stability.

The optical characterization of GaN-ZnO nanowires showed significant band gap reduction with increasing ZnO content. As band gap decreased from 3.4 eV (pure GaN) to 2.6 eV, shifting the absorption edge from the ultraviolet (365 nm) to the visible region (~477 nm). This is attributed to the incorporation of $Zn2^{+}$ and $O2^{-}$ ions, which introduce Zn 3d and O2p states into the valence band, enhancing the hybridization with N2p orbitals. Similar redshifts due to band gap narrowing have been reported by Ahn et al. (2016), who used ZnO incorporation in GaN-based heterostructures to improve visible light absorption [6, 15]. This band gap tunability is vital for photodetector applications under ambient lighting. Compared to conventional phototransistors based on wide- bandgap semiconductors such as GaN, GaN-ZnO nanowires developed here offer broader spectral sensitivity, improving their utility in practical optoelectronic systems. Our results are consistent with previous findings by Liu et al. (2016), who reported that optimized thermal processing is essential for achieving high responsivity in ReS_2 nanowire phototransistors [8]. Our findings reinforce that balanced thermal budget is critical for tailoring the microstructure and carrier mobility in nanomaterials used for photodetection.

The incorporation of AgNPs onto GaN-ZnO nanowires led to a substantial improvement in device performance, decorated device showed enhanced photocurrent of 9.44 nA, responsivity of 131.7 A/W, detectivity of 3.5×10^{11} Jones and reduced response time of 5.9 ms. Stability also improved markedly, with current retention rising from 78.5% to 92.2% after five cycles. These improvements are attributed to LSPR induced by AgNPs, which increases the local electromagnetic field intensity and enhances photon absorption in the channel. Comparable enhancements have been demonstrated by Hu et al. (2014), where Ag-decorated GaTe nanosheet phototransistors exhibited elevated responsivity due to increased carrier generation near the metal– semiconductor interface [11, 16]. Our study confirmed that plasmonic decoration is a practical strategy to boost light-matter interaction and improve the responsivity and stability of nanowire-based phototransistors.

The WS_2–InGaZnO heterojunction phototransistor outperformed both individual layers, achieved the highest photocurrent (9.6 nA), on/off ratio (10^4), responsivity (122.5 A/W), detectivity (3.8×10^{11} Jones) and best cycle stability (91.7%). These improvements stem from the synergistic band alignment at the heterointerface. WS_2, acts as a strong light-absorbing layer due to its direct band gap and high absorption coefficient, while InGaZnO provides high mobility and low carrier recombination losses for effective charge transport [17-18]. This heterostructure design mirrors the findings of Ye et al. (2016), who demonstrated enhanced near-infrared photodetection using MoS_2/black phosphorus heterojunctions, showing that 2D–oxide hybrid heterostructures can combine the benefits of spectral absorption and carrier mobility [5]. Similarly, our results validate that WS_2– InGaZnO heterojunctions not only expand spectral response but also improve carrier extraction efficiency and device durability.

When compared to state-of-the-art phototransistors, the devices fabricated in this work show competitive or superior performance. For example: Few-layer ReS_2 devices achieved responsivity up to ~88,600 A/W under specific conditions [7, 19], but such extreme values often come at the cost of slow response times and large dark currents. Hybrid perovskite phototransistors have shown high responsivity (~320 A/W) and fast response, but face long-term stability issues [7]. MoS_2 and HfS_2-based devices reported by Choi et al. (2012) and Kai et al. (2015) achieved responsivity in the range of 80– 890 A/W with varied response times [4, 14]. In contrast, the GaN-ZnO and WS_2–

InGaZnO phototransistors in this study maintained favorable balance of high responsivity (>120 A/W), fast response (<6.5 ms), low dark current (<0.4 nA) and improved operational stability, making them well- suited for real-world optoelectronic systems such as environmental sensors and high-speed optical switches.

The cyclic stability tests demonstrated reliable device performance over multiple on/off cycles for both Ag- decorated and heterojunction-based devices. Stability increased by ~14% in AgNP-decorated nanowire devices and ~26% in WS_2–InGaZnO heterojunctions compared to their pristine counterparts. This is crucial for practical applications where devices are repeatedly exposed to fluctuating light conditions. Similar observations were made by Ahn et al. (2016), who noted enhanced durability in multilayer phototransistors with passivation layers [6, 20, 21].

While this study successfully demonstrates high-performance phototransistors with enhanced metrics, several challenges remain. The alignment of individual nanowires for scalable device fabrication remains non-trivial and requires further optimization through techniques such as dielectrophoresis or Langmuir–Blodgett assembly. Additionally, integration with flexible or transparent substrates could further broaden application potential in wearable electronics or optical biosensors. The stability of plasmonic enhancement under prolonged operation and environmental exposure must also be assessed. Future work could explore alternative metal nanoparticles and protective capping layers to enhance long-term durability.

Conclusion

This study successfully demonstrated the fabrication and performance optimization of high-performance phototransistors based on GaN-ZnO solid solution nanowires and WS_2–InGaZnO heterojunctions. Band gap engineering through ZnO incorporation effectively extended the absorption edge from the UV to visible range, enhancing photoresponse. Optimization of synthesis temperature at 850 °C yielded the best trade-off between crystallinity, carrier mobility and response speed. Plasmonic enhancement using Ag nanoparticles significantly improved photocurrent, responsivity, and response time due to localized surface plasmon resonance effects. Furthermore, WS_2–InGaZnO heterojunction device exhibited superior optoelectronic characteristics—including a high on/off ratio (10^4), responsivity (122.5 A/W), and detectivity (3.8×10^{11} Jones) attributed to efficient carrier separation and transport across the heterointerface. These results highlighted the potential of combining nanoscale material engineering and hybrid device architectures to develop next-generation, broadband and stable photodetectors for practical optoelectronic applications.

REFERENCES

[1] C. Sharma, N. Sharma, P. Sharma, and V. Kumar, "A review of BJT-based phototransistor," *Int. J. Eng. Res. Technol.*, vol. 3, no. 4, pp. 306–310, Apr. 2014.

[2] T. P. I. Saragi, R. Pudzich, T. Fuhrmann, and J. Salbeck, "Organic phototransistor based on intramolecular charge transfer in a bifunctional spiro compound," *Appl. Phys. Lett.*, vol. 84, pp. 2334–2336, 2004.

[3] J. Lu *et al.*, "Ultrasensitive phototransistor based on K-enriched MoO_3 single nanowires," *J. Phys. Chem.* C, vol. 116, pp. 22015–22020, 2012.

[4] W. Choi *et al.*, "High-detectivity multilayer MoS_2 phototransistors with spectral response from ultraviolet to infrared," *Adv. Mater.*, vol. 24, pp. 5832–5836, 2012.

[5] L. Ye, H. Li, Z. Chen, and J. Xu, "Near-infrared photodetector based on MoS_2/black phosphorus heterojunction," 2016.

[6] C. H. Ahn *et al.*, "Highly repeatable and recoverable phototransistors based on multifunctional channels of photoactive CdS, fast charge transporting ZnO, and chemically durable Al_2O_3 layers," *ACS Appl. Mater. Interfaces*, vol. 8, 2016.

[7] F. Li, "Ambipolar solution-processed hybrid perovskite phototransistors," *Nat. Commun.*, vol. 6, Art. no. 8238, 2015.

[8] E. Liu *et al.*, "High responsivity phototransistors based on few-layer ReS_2 for weak signal detection," *Adv. Funct. Mater.*, vol. 26, pp. 1938–1944, 2016.

[9] O. Lopez-Sanchez *et al.*, "Ultrasensitive photodetectors based on monolayer MoS_2," *Nat. Nanotechnol.*, vol. 8, pp. 497–501, 2013.

[10] C. Rocha Leão and V. Lordi, "Ab-initio guided optimization of layered semiconductors (GaTe, GaSe) for radiation detection applications," in *APS Meeting*, 2010.

[11] P. Hu *et al.*, "Highly sensitive phototransistors based on two-dimensional GaTe nanosheets with direct bandgap," *Nano Res.*, vol. 7, pp. 694–703, 2014.

[12] B. Y. Zhang *et al.*, "Broadband high photoresponse from pure monolayer graphene photodetector," *Nat. Commun.*, vol. 4, Art. no. 1811, 2013.

[13] G. Fiori *et al.*, "Electronics based on two-dimensional materials," *Nat. Nanotechnol.*, vol. 9, pp. 768–779, 2014.

[14] X. Kai *et al.*, "Ultrasensitive phototransistors based on few-layered HfS_2," *Adv. Mater.*, vol. 27, 2015.

[15] T. Hirai *et al.*, "Origin of visible light absorption in GaN-rich $(Ga_{1-x}Zn_x)(N_{1-x}O_x)$ photocatalysts," *J. Phys. Chem. C*, vol. 111, pp. 10295–10300, 2007.

[16] M. Asad, S. Salimian, M. H. Sheikhi, and M. Pourfath, "Flexible phototransistors based on graphene nanoribbon decorated with MoS_2 nanoparticles," *Sens. Actuators A, Phys.*, vol. 232, pp. 285–291, Aug. 2015.

[17] J. Li *et al.*, "Type-II superlattice-based heterojunction phototransistors for high-speed applications," *Infrared Phys. Technol.*, vol. 108, Art. no. 103350, Aug. 2020.

[18] J. Li, A. Dehzangi, and M. Razeghi, "Performance analysis of infrared heterojunction phototransistors based on Type-II superlattices," Center for Quantum Devices, Northwestern Univ., Evanston, IL, USA, Tech. Rep., pp. 1–11.

[19] K. Thakar *et al.*, "Multilayer ReS_2 photodetectors with gate tunability for high responsivity and high-speed applications," *ACS Appl. Mater. Interfaces*, vol. 10, no. 42, pp. 36424–36433, Sep. 2018.

[20] A. Cao, E. J. Sudhölter, and L. C. de Smet, "Silicon nanowire-based devices for gas-phase sensing," *Sensors*, vol. 14, no. 1, pp. 245–271, 2013.

[21] L. A. P. Santos, "An overview on bipolar junction transistor as a sensor for X-ray beams used in medical diagnosis," *Sensors*, vol. 22, no. 5, Art. no. 1923, 2022

.